THE ASTROPHYSICAL JOURNAL, 324:823–839, 1988 January 15

RED VARIABLES IN GLOBULAR CLUSTERS: THEIR CLASSIFICATION AND EVIDENCE FOR MASS LOSS[1]

JAY A. FROGEL[2]
Kitt Peak National Observatory, National Optical Astronomy Observatories[3]
AND
J. H. ELIAS[2]
California Institute of Technology, and Cerro Tololo Inter-American Observatory, National Optical Astronomy Observatories[3]
Received 1987 April 17; accepted 1987 July 13

ABSTRACT

Long-period variables (LPVs) in globular clusters are shown to have excess infrared emission at 3.5 and 10 μm and strong H_2O absorption. These characteristics are evidence for circumstellar dust shells and extended atmospheres. The LPVs are asymptotic giant branch members with luminosities greater than that at which core helium flash is expected to occur. Just below the core helium flash limit is a group of red variables which are peculiar in that they lie significantly to the blue of their parent cluster giant branch and have excess emission and absorption similar to, though weaker than, that seen in the LPVs. There do not appear to be any other cluster members, variable or nonvariable, which have these characteristics of the LPVs or the peculiar variables.

The presence of circumstellar shells in LPVs in globular clusters with metallicities up to 10 times less than solar and their absence in non–LPV cluster giants of similar luminosity and temperature and similar or greater metal abundance agrees with theoretical predictions that stellar pulsation will considerably increase (and may in fact dominate) the mass-loss rate over that predicted from the effects of radiation pressure on grains alone. Typical values we derive for dM/dt are $5 \times 10^{-6}\ M_{\odot}\ \mathrm{yr}^{-1}$. Finally, we find some indication that the dust around the globular cluster variables may be relatively poor in silicates.

Subject headings: clusters: globular — infrared: sources — stars: circumstellar shells — stars: long-period variables — stars: mass loss

I. INTRODUCTION

In the past 4 years there have been a number of new, extensive investigations of red variables. Feast *et al.* (1982) examine trends in the *JHKL* colors of galactic field variables with a data base of several hundred stars. Glass and Feast (1982*b*) and Wood, Bessell, and Fox (1983) examine the properties of long-period variables (LPVs) in the Magellanic Clouds. Feast (1985), Whitelock (1986), and Menzies and Whitelock (1985) discuss the period-luminosity relation for globular cluster variables. Lloyd Evans (e.g., 1983*b*, 1984) has presented a series of papers on the optical spectra of red giants in globular clusters, both variable and nonvariable. There has also been a spate of studies of LPVs in the Galactic bulge (e.g., Glass and Feast 1982*a*; Wood and Bessell 1983; Jones, Hyland, and Robinson 1984; Frogel and Whitford 1987; and Whitelock, Feast, and Catchpole 1986).

Because of the sensitivity of posthorizontal branch evolution to both stellar envelope mass and total mass, it is especially important to determine mass-loss rates for globular cluster giants. Even the simple question of whether or not such mass loss is seen has been difficult to answer. For example, Cohen (1976) and Mallia and Pagel (1980) interpreted the weak, blue-shifted Hα emission lines seen in some globular cluster red giants as arising from a steady mass outflow. Dupree, Hartmann, and Avett (1984), on the other hand, argue that such emission can come from a static stellar chromosphere with no mass loss.

The purpose of this paper is twofold: to reexamine the classification scheme for red variables in globular clusters and to investigate evidence for mass loss in these stars. By "red variable" we will imply a variable that lies on or near a globular cluster's giant branch. A common way of estimating mass-loss rates in cool stars is to use a formula such as that given by Reimers (1975). However, large-amplitude variables and stars that differ significantly from solar metal abundance are essentially absent from the data base he used to derive his formula. Clearly, relatively accurate values can be determined for important physical parameters for red variables from a study of those that lie in globular clusters.

In a previous paper (Frogel 1983, hereafter Paper I), infrared observations of more than 50 red giant variables in globular clusters were used to investigate their evolutionary state and draw some qualitative conclusions about the mass loss. The data base of Paper I has been significantly enlarged by obtaining infrared observations for an additional 20 red variables, with emphasis placed on acquiring data at 3.5 and 10 μm. These longer wavelengths are particularly valuable for determining the presence of circumstellar dust shells. Infrared data are now available for nearly every known cluster LPV and "peculiar" variable; the latter appellation is assigned to those variables which lie significantly to the blue of the mean giant branches in their respective clusters in both $V-K$ and $J-K$ (Paper I). Feast (1973) defined cluster LPVs as "red giants with long periods (generally greater than 100 days), large ampli-

[1] Based on observations made at Cerro Tololo Inter-American Observatory.
[2] Guest Investigator, NASA Infrared Telescope Facility, Hawaii.
[3] Operated by the Associated Universities for Research in Astronomy, Inc., under contract with the National Science Foundation.

TABLE 1

NEW CITO OBSERVATIONS OF CLUSTER VARIABLES

Cluster	Sta	Reddening Corrected Photometry[a] K_0	$(V-K)_0$	$(J-K)_0$	$(H-K)_0$	$(K-L)_0$	$(K-[10])_0$	H_2O	CO	Physical Parameters[a] BC_K	M_{bol}	Type[b]	P	Notes
NGC 104	V1	6.18	6.3	1.19	0.45	0.50	1.42 (11)	0.74	0.15	3.03	-3.93	LPV	212	4,5
(47 Tuc)		6.63	...	1.12 (3)	0.45	0.62 (5)	1.98 (12)	0.68 (6)	0.095	...	...	...	...	1
		6.49 (12)	...	1.15 (14)	0.43 (5)	0.43 (5)	1.53 (19)	0.92 (3)	0.205	...	...	...	...	23,24
		6.38	...	1.36	0.62	0.28	1.49 (15)	...	...	...	...	...	...	25
	V2	5.86	4.0	1.10	0.35	0.44	0.71 (14)	0.44	0.135	2.70	-4.58	LPV	203	4,5
		6.49	...	1.06 (14)	0.42 (4)	0.42 (5)	1.68 (8)	0.74 (3)	0.16	...	...	...	...	23,24
		6.46	...	1.13	0.45	0.40	1.45 (13)	...	...	...	...	...	...	25
	V3	6.34	7.5	1.21	0.42	0.43	0.89 (23)	0.61	0.14	3.12	-3.68	LPV	192	4,5
		6.06 (3)	...	1.03	0.25	0.31 (4)	1.08 (12)	0.40 (6)	0.24	...	...	...	...	1
		6.71 (12)	...	0.87 (14)	0.24 (5)	0.36 (5)	1.95 (18)	0.40 (3)	0.20	...	...	...	...	23,24
		6.15	...	1.01	0.31	0.31	1.00 (15)	...	...	...	...	...	...	25
	V4	6.57	6.7	1.15	0.34	0.42	1.36 (15)	0.49	0.11	3.04	-3.53	LPV?	82	4,5
		6.31 (12)	...	0.89 (14)	0.24 (4)	0.36 (5)	1.19 (20)	0.28 (3)	0.15	...	...	...	...	23,24
	V19	7.50	3.7	0.97 (3)	0.19	0.13 (5)	...	0.12 (6)	0.12	2.60	-3.04	Pec	...	1,5
NGC 288	V1	8.56 (5)	3.9	0.92 (3)	0.12 (3)	0.23 (4)	...	0.06 (5)	0.11	2.61	-3.47	...	103	1,5
NGC 362	V2	8.68 (5)	3.9	0.92 (3)	0.20 (3)	0.28 (5)	...	0.10 (6)	0.075	2.62	-3.48	...	90	1,5
NGC 1261	V15	9.74	...	0.93 (3)	0.16	0.26 (6)	...	0.06 (5)	0.11	2.62	-3.43	...	...	1
NGC 1904	V2	10.02 (3)	3.1	0.83(3)	0.14	0.14 (6)	...	0.07 (6)	0.06	2.39	-3.19	...	...	1,5
NGC 4833	V9	8.12	3.0	0.67	0.11	0.16	0.62 (21)	0.05	0.02	2.31	-3.27	Pec	87.7	3,5
NGC 5897	V5	9.77	3.3	0.79	0.13	0.12	...	0.04	0.015	2.43	-3.26	...	54.5	3,5
NGC 5927	V3	7.61	~7	1.29	0.57	0.62	1.35 (17)	0.955	0.115	3.11	-3.71	LPV	312	5
NGC 6121	V4	5.86	3.3	0.76	0.18	0.23	0.93 (17)	0.055	-0.01	2.42	-3.32	Pec	60	2,3,4,5
(M4)	V13	6.19	3.6	0.90	0.16	0.14	0.48 (17)	0.05	0.085	2.55	-2.86	...	40	2,3,4,5
NGC 6356	V1	8.53	5.3	1.13	0.38	0.55	...	0.385	0.08	2.90	-4.58	LPV	230.6	6
	V2	10.14	4.8	1.00	0.18	...	...	0.085	0.17	2.80	-3.07	...	...	7
	V3	9.47	5.8	1.19	0.54	0.59	...	0.885	0.145	3.00	-3.54	LPV	220.0	8
	V4	8.82	5.5	1.09	0.31	0.47	...	0.265	0.19	2.91	-4.28	LPV	207.3	9
	V5	8.73	5.4	1.05	0.30	0.42	...	0.455	0.23	2.89	-4.39	LPV	219.8	10
NGC 6388	V1	8.59	...	0.99	0.27	0.44	...	0.27	0.11	2.66	-4.26	LPV	...	11
	V2	8.10	...	0.96	0.29	0.49	...	0.50	0.20	2.81	-4.60	LPV	...	11
	V3	8.90	4.6	1.11	0.21	0.21	...	0.11	0.14	2.81	-3.80	...	...	12
	V4	8.37	...	1.18	0.42	0.58	...	0.44	0.115	2.99	-4.15	LPV	...	11
	V8	9.74	2.8	0.89	0.23	0.35	...	0.12	0.025	2.32	-3.45	Pec	...	12,13
NGC 6637	V1	8.54	3.7	1.01	0.21	0.21	...	0.20	0.195	2.61	-3.71	...	...	19
(M69)	V3	8.46	4.2	0.98	0.18	0.18	...	0.11	0.14	2.69	-3.71	Pec	...	5,20
	V4	7.98	6.9	1.19	0.41	0.58	...	0.76	0.185	3.05	-3.83	LPV	196	5,21
	V5	8.01	(6.9)	1.17	0.49	0.70	...	0.64	0.08	3.04	-3.81	LPV	195	22
	V6	8.18	5.55	1.10	0.23	0.22	...	0.16	0.16	2.93	-3.75	...	...	5
	V7	8.60	4.4	1.04	0.19	0.15	...	0.08	0.16	2.76	-3.50	...	...	5
NGC 6712	V2	8.19	3.6	0.73	0.18	0.33	...	0.47	0.185	2.49	-3.48	Pec	104.6	14
	V7	7.01	4.1	0.96	0.28	0.48	...	0.35	0.205	2.66	-4.49	LPV	190.5	15
	V8	8.30	3.0	0.91	0.21	0.26	...	0.20	0.19	2.39	-3.47	Pec	117.0	16
	V10	8.07	4.4	1.01	0.18	0.18	...	0.09	0.16	2.75	-3.34	...	174	17
	V21	8.22	4.2	0.98	0.15	0.17	...	0.10	0.145	2.70	-3.24	...	...	18

[a] Reddening values and distance moduli for clusters with previously published infrared data are the same as taken from those used in the original sources. For clusters not previously observed in the infrared, these two quantities were derived according to the precepts in Frogel, Persson, and Cohen 1983. For convenience, we give here values of $E(B-V)_0$, $(m-M)_0$, and [Fe/H] for each cluster. The latter quantity is from Zinn and West 1984. NGC 104—0.04, 13.14, −0.71; NGC 288—0.02, 14.64, −1.40; NGC 362—0.04, 14.78, −1.27; NGC 1261—0.01, 15.79, −1.31; NGC 1904—0.00, 15.60, −1.69; NGC 4833—0.36, 13.70, −1.86; NGC 5897—0.06, 15.46, −1.68; NGC 5927—0.46, 14.43, −0.30; NGC 6121—0.36, 11.60, −1.33; NGC 6356—0.27, 16.01, −0.62; NGC 6388—0.35, 15. 51, −0.74; NGC 6637—0.17, 14.86, −0.59; NGC 6712—0.39, 14.16, −1.01.

Values of these quantities for clusters in Table 1 of Paper I but not in this table are NCG 1851—0.02, 15.44, −1.36; NGC 5024—0.03, 16.24, −2.04; NGC 5139 (W Cen)—0.11, 13.60, −1.59; NGC 6171—0.38, 13.71, −0.99; NGC 6352—0.25, 13.55, −0.51; NGC 6553—0.79, 13.62, −0.29; NGC 6656—0.36, 12.45, −1.75; NGC 7006—0.05, 18.12, −1.59.

[b] For variables that are not LPVs or Pecs, no type is given.

1. These data were obtained in 1984 Nov and Dec. The photometry is not of particularly high accuracy because the nights had variable transmission. Except for the LPVs, the variation at K is <0.1 mag, so only minor adjustments were made to the previously used $V-K$ values.
2. The $(K-L)_0$ value for these stars in Paper I were inadvertently not corrected for reddening. The $(K-L)_0$ values in Paper I should be 0.23 and 0.14 for V4 and V13, respectively.
3. Because of small amplitude, $(V-K)_0$ assumed to be same as in Paper I.
4. The [10 μm] data were obtained on same nights as data published in Frogel, Persson, and Cohen 1981 for 47 Tuc; 1983 for M4.
5. Also listed in Paper I.
6. Optical data from Table III of Clement and Hogg 1977. Assumed $(B-V)_0 = 1.6$; ϕ for IR data $= 0.99$.

1988ApJ...324..823F

tudes (Δm greater than ~ 2.5 mag), and Me spectra," consistent with Hogg's (1973) classification criteria followed here.[4] A preliminary discussion of the new results is given in Frogel (1985*a*).

II. THE DATA AND PHYSICAL PARAMETERS

a) New CTIO Data

Table 1 contains the new data obtained with the Ga:Ge bolometer and the D3 InSb system at CTIO on the 1.5 and 4 m telescopes. The *JHKL* data are on the "CIT/CTIO" system (Elias *et al.* 1982), while the 4.8 (*M*) and 10 (*N*) μm data are on the natural photometric system of the InSb and bolometer systems, respectively. Unless otherwise noted in the table, all observations for a star were obtained as close together in time as possible—usually on the same night—so that these new data superseded previously published data. Also note the correction to the Paper I data for V4 and V13 in M4. For completeness, the data for the variables in NGC 6712 are repeated from Frogel (1985*b*). Corrections for extinction and reddening have been applied following Frogel, Persson, and Cohen (1983, hereafter FPC). The values used are summarized in the notes to Table 1; sources and further details are given in FPC.

b) IRTF Data

Observations were made during 1980 July–August with the IRTF bolometer and InSb detector systems in Hawaii. The data are presented in Table 2. Measurements at *J*, *H*, and *K* have been transformed to the "CIT/CTIO" system (Elias *et al.* 1982) with the equations

$$(J-K)_{\rm CIT} = 0.93(J-K)_{\rm IRTF}\,, \qquad (1a)$$

$$(H-K)_{\rm CIT} = 0.92(H-K)_{\rm IRTF}\,. \qquad (1b)$$

These transformations differ from those presented by Humphreys, Jones, and Sitko (1984); the differences are presumably due to alterations made in the IRTF dectector systems during the intervening period. The longer wavelength data were left on the IRTF natural system; the $K-L$ colors appear to be close to those which would have been measured on the "CIT/CTIO" system (note that we did not use a longer wavelength L' filter); there are no obvious differences between the CTIO and IRTF data at 4.8 and 10 μm. The 10 and 20 μm data were all obtained within one or two nights of the 1.2–4.8 μm data. The data in Table 2 have been reddening corrected following Table 1 (details given in the notes).

[4] Alternatively, we have Pickering's (1881) succinct definition of LPVs as "stars undergoing great variations in light in periods of several months or years." On page 96 of their monograph, Payne-Gaposchkin and Gaposchkin (1938) discuss in some detail the difficulty of precisely defining an LPV, but conclude that "all the criteria taken together will define a long-period variable with considerable success."

c) Physical Parameters

Bolometric magnitudes and effective temperatures for the variables are from the sources cited in Paper I or calculated as discussed in these sources. Distance moduli are from FPC or as noted in Tables 1 and 2. As emphasized in Paper I and in Frogel, Persson, and Cohen (1981, 1983), $J-K$ cannot be used to estimate accurate temperatures for the coolest stars because (*a*) it is quite insensitive to temperature changes for the regime in which these stars lie, and (*b*) there are large, unpredictable, and generally not understood blanketing effects on $J-K$, particularly due to H_2O, at the relevant temperatures (cf. discussion by Frogel and Whitford 1987 and in § V below). The resulting uncertainties in the temperature scale, though, are still not great enough to affect the discussion of mass loss later in the paper.

III. LUMINOSITIES OF THE VARIABLES

Figure 1 illustrates the dependence of the bolometric magnitudes of the variables on cluster metallicity for the data from Table 1 and Paper I. The thin line illustrates the dependence of luminosity at the time of core He flash on metallicity and is based on the models of Sweigart and Gross (1978); it is taken from Figure 6 of Frogel, Cohen, and Persson (1983, hereafter FCP). Figure 1 demonstrates that variables significantly more luminous than core He flash are strictly confined to metal-rich clusters. NGC 6712 with a [Fe/H] $= -1.0$ is the most metal-poor cluster with a luminous variable.

All but six of the variables above the core He flash line are LPVs. Of these six, three are from M69 whose distance modulus is probably overestimated (FCP); a fourth is from NGC 6388, a poorly studied, highly reddened cluster; a fifth, NGC 6352–L36, has not previously been recognized optically as an LPV because of limited data (T. Lloyd Evans, private communication); the sixth, V4 in 47 Tucanae, is a borderline LPV (Frogel, Persson, and Cohen 1981; Paper I). The only LPV lying just below the core He flash line is NGC 6356 V3. This star was observed only once in the infrared, probably near minimum light as judged from its optical appearance. Data from Menzies and Whitelock (1985) show this star to be as

NOTES TO TABLE 1—*Continued*

7. Same as note 6, except took mean *B* mag to get $(V-K)_0$.
8. Same as note 6, except ϕ for IR data = 0.72.
9. Same as note 6, except ϕ for IR data = 0.18.
10. Same as note 6, except ϕ for IR data = 0.11.
11. No periods or magnitudes are available for the LPVs in NGC 6388.
12. Mean *V* mag were taken from Lloyd Evans and Menzies 1977.
13. Lloyd Evans and Menzies 1977. Note that NGC 6388-V8 may be similar to V19 in 47 Tuc.
14. Period and magnitude data from Sandage, Smith, and Norton 1966. Mean *V* used to compute $(V-K)_0$ ($\equiv$ AP Sct).
15. Same as note 14, except ϕ for IR data near 0.14 ($\equiv$ CM Sct).
16. Same as note 14, except IR data taken near maximum light.
17. Same as note 14, except IR data near $\phi = 0.6$.
18. Mean *V* magnitude used from Lloyd Evans and Menzies 1977.
19. Take mean *B* magnitude from Hogg 1973. Assume $(B-V)_0 = 1.3$.
20. Use same $(V-K)_0$ as in Paper I.
21. IR data obtained probably near minimum.
22. Assume $(V-K)_0$ same as M69-V4.
23. Observed 1980 Sep 26.
24. $(K-M)_0$ for V1, 2, 3, and 4 are 0.69(16), 0.69(16), 0.84(16), and 0.65(16), respectively.
25. Observed 1980 Oct 21.

TABLE 2

IRTF Observations of Cluster Stars

Cluster	Star	Reddening Corrected Photometry[a]							Physical Parameters[a]		
		K_o	$(V-K)_o$	$(J-K)_o$	$(H-K)_o$	$(K-L)_o$	$(K-M)_o$	$(K-[10])_o$	BC_K	M_{bol}	Var?
NGC 6121 (M4)	V4	5.79	3.3	0.76 (3)	0.17	0.26 (4)	0.45 (5)	0.82 (6)[b]	2.41	-3.40	Yes-Pec
	V13	6.22	3.6	0.90 (3)	0.14	0.12 (4)	0.07 (8)	0.06 (10)	2.54	-2.84	Yes
	1514	5.65	4.1	0.99 (3)	0.18	0.11 (4)	-0.01 (6)	0.30 (9)	2.69	-3.26	No
	4611	5.57	4.35	1.06 (3)	0.18 (3)	0.08 (4)	-0.01 (6)	-0.08 (8)	2.76	-3.27	No
	4613	5.60	4.11	1.05 (3)	0.19 (3)	0.09 (4)	-0.08 (6)	-0.27 (11)	2.72	-3.28	No
	3209	6.34	3.47	0.91 (3)	0.14 (3)	0.05 (4)	-0.08 (7)	...	2.52	-2.74	No
NGC 6205 (M13)	IV-25	8.52	3.48	0.89 (3)	0.14 (3)	0.09 (3)	0.21 (17)	0.48 (49)	2.52	-3.29	No
NGC 6341 (M92)	III-13	8.89	3.06	0.77	0.12	0.09 (4)	-0.49 (48)	<0.4	2.35	-3.20	No
NGC 6656 (M22)	V5	6.72	3.2	0.74 (3)	0.11	0.05 (4)	-0.05 (8)	0.22 (9)	2.39	-3.34	Yes
	V8	6.93	2.9	0.63 (3)	0.13	0.18 (4)	0.09 (6)	0.83 (9)	2.25	-3.27	Yes-Pec
	V9	6.70	3.5	0.82 (3)	0.13	0.03 (4)	-0.17 (8)	0.24 (10)	2.50	-3.25	Yes
	III-3	6.71	3.20	0.83 (3)	0.11	0.03 (4)	-0.19 (10)	-0.08 (27)	2.42	-3.32	No
	III-14	6.69	3.37	0.82 (3)	0.13	0.03 (4)	-0.03 (7)	0.04 (18)	2.47	-3.29	No
NGC 6838 (M71)	29	6.49	5.6	1.04	0.23	0.15 (4)	0.12 (7)	0.10 (10)	2.93	-3.48	Yes
	B	6.86	4.58	1.02	0.17	0.00 (4)	-0.27 (8)	0.36 (14)	2.78	-3.26	No
	30	7.84	3.48	0.95	0.15	0.08 (4)	-0.23 (13)	-0.05 (30)	2.54	-2.52	No
	113	7.93 (3)	3.84	0.93 (4)	0.17 (3)	0.00 (5)	-0.20 (13)	0.06 (37)	2.61	-2.36	No

[a] For clusters not in Table 1, values for $E(B-V)_0$, $(m-M)_0$, and [Fe/H] are: NGC 6205—0.03, 14.33, −1.65; NGC 6341—0.02, 14.44, −2.24; NGC 6656—0.36, 12.45, −1.75; NGC 6838—0.25, 12.90, −0.58.

[b] $(K-[20])_0 = 1.86$ (23).

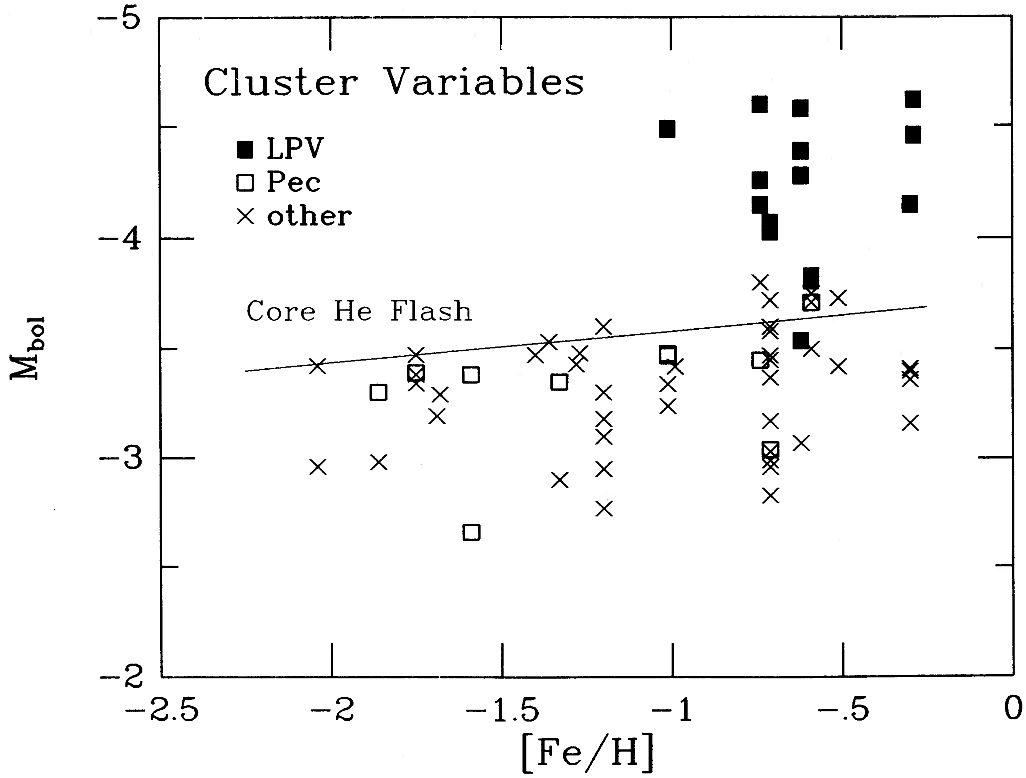

FIG. 1.—Luminosity vs. metallicity for globular cluster variables with data from this paper and Paper I. The line for core He flash, which marks the upper limit of the first giant branch, is based on the models of Sweigart and Gross (1978). The "pec" variables are those which lie a few tenths of a magnitude to the blue of their cluster's giant branch in $V-K$ and $J-K$

luminous as V4 and V5 in the same cluster, i.e., with an M_{bol} about 0.8 mag brighter than reported here. It is also interesting to note that, of the 10 "peculiar" variables, eight have M_{bol} within 0.2 mag of the He core flash luminosity, generally slightly below it.

With a few exceptions all known red giant variables in the present sample of clusters were observed. In agreement with Welty (1985) and with Paper I, Figure 1 shows that most of the variables regardless of type have $M_{bol} < -3.0$. There is no correlation evident between minimum luminosity needed for variability with metallicity.

Photometry of most of the known luminous giants in a large sample of globular clusters plus infrared scans of a subset of these clusters did not reveal any nonvariable star to be more luminous than the theoretically predicted location of core He flash for each cluster (FPC). *We conclude that the most luminous (brighter than core He flash) stars in Galactic globular clusters, independent of metallicity, are variables; that these variables are probably all LPVs; and that they are a population of stars found only in relatively metal-rich clusters.*

IV. $K-L$ AND $K-N$ COLORS OF THE VARIABLES

a) $K-L$

If a star has a circumstellar dust shell with a color temperature of 600 K or greater, it will have excess infrared emission in the L band. Figure 2 (with data for twice as many variables as in Fig. 2 of Paper I) shows the dependence of $K-L$ on $J-K$ for red variables in globular clusters. The important result from Figure 2 is that many of the variables have significant excess emission at L for their $J-K$ color, i.e., their $K-L$ colors are several tenths of a magnitude redder *at the same* $J-K$ than those of nonvariable field giants. Specifically, *all* LPVs have L excesses of 0.2 to 0.4 mag; the majority—six out of eight—of the peculiar variables (Pecs) have excess emission in the L band of up to 0.2 mag in spite of their relatively blue $J-K$ colors; and (with only a few exceptions) non–LPV and non-peculiar variables do not have excess emission at L. The LPVs stand apart from all other variables (the two reddest, in $K-L$, "non–LPVs" are again 47 Tuc V4 and NGC 6352–L36); this clear distinction between the LPVs and other types of stars in Figure 2 is qualitatively similar to that seen for the variables in "Baade's window" (Frogel and Whitford 1987) and in the field (Feast *et al.* 1982) and is consistent with Wood's (1979) theoretical treatment of the effects of pulsation on mass loss as discussed in § VII*b*.

Absorption by H_2O makes K magnitudes fainter by an amount equal to 0.2 × [H_2O] (Frogel, Persson, and Cohen 1981). Since $K-L$, and $H-K$, and H_2O are highly correlated for all three groups of variables (see, e.g., Fig. 3) correction for this effect will tend to preferentially decrease the mean $K-L$ colors of the LPVs by about 0.1 mag. Nevertheless, the separation between the groups of stars in Figure 2 remains.

The referee has suggested that the apparent $K-L$ excess for the stars in Figure 2 is due not to circumstellar dust emission, but to a much cooler photospheric temperature in many of the variables than in the nonvariables. The constancy of $J-K$ is claimed to arise from the competing effects of lower temperature and stronger H_2O absorption. As we have stated in the previous paragraph, application of the H_2O correction does not remove the appearance of excess L flux from many of the stars in Figure 2. In any case for the warmer "Pec" variables such as M4–V4 there are nonvariable, nonexcess objects

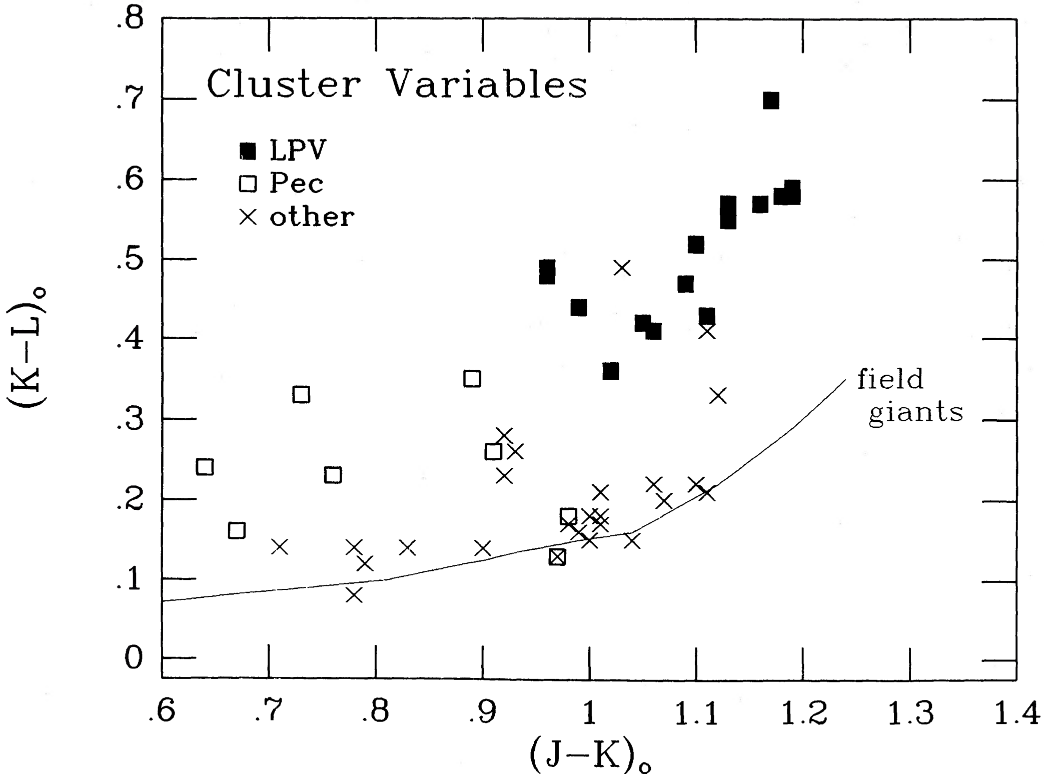

FIG. 2.—$K-L$ vs. $J-K$ for globular cluster variables as in Fig. 1. The mean relation between $J-K$ and $K-L$ is taken from Paper I.

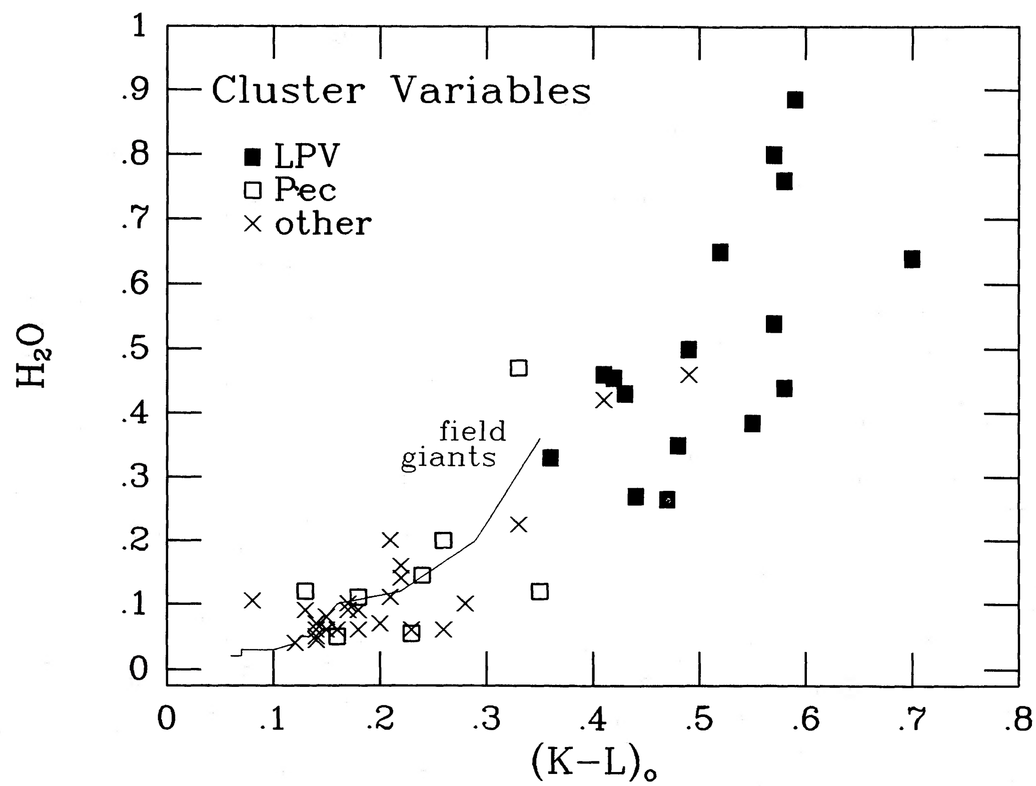

FIG. 3.—H_2O vs. $K-L$ for globular cluster variables as in Figs. 1 and 2

with essentially identical infrared and optical properties *except* for the presence of excess L and 10 μm emission. Although it is probably not meaningful to predict blackbody colors for the stars from effective temperatures, *differential* colors can serve as a guide to the size of the temperature changes required. For example around 3000 K any decrease in $K-L$ would require a decrease in $J-K$ about twice as large. A change in $K-L$ of 0.2 mag would require a change in temperature of 500–1000 K. Similarly to explain the observed $K-[10]$ excess in terms of reduced photospheric temperature, one would need a reduction of over 500 K from what would be predicted from near-infrared colors. In both of these cases one would have to have an ad hoc blanketing law that would just compensate for the effects on $J-K$. Excess emission due to circumstellar dust is, to us, a more plausible explanation for the observations.

b) 10 μm *Data*

Although data at 10 μm are more difficult to obtain than those at L, they can provide a clearer delineation between photospheric and circumstellar emission. This section will examine such data obtained for the globular cluster giants.

Figure 4 shows the correlation between $K-L$ and $K-[10]$ for globular cluster red giants, variables from "Baade's window" (Frogel and Whitford 1987), and red supergiants from the Magellanic Clouds (Elias, Frogel, and Humphreys 1985). The "Baade's window" stars are of an age comparable to the globular cluster stars but with a mean metallicity probably an order of magnitude greater (Whitford and Rich 1983; Rich 1986; but see Wood and Bessell 1983 for a significantly different age estimate). The supergiants are quite young but probably have a metallicity comparable to that of the most metal-rich of the globular clusters.

The two colors in Figure 4 are reasonably well correlated. In fact, the real correlation is better than it appears in this figure. For values of $K - [10] > 0.7$ the range in H_2O is from 0.6 to 1.0 mag. Figure 5 shows the effect of applying a correction of $0.2 \times [H_2O]$ to the K magnitudes in Figure 4 (corrected K magnitudes are denoted with a subscripted "c"). The scatter *within a given sample* is reduced to a size comparable to the measuring errors. The cluster and bulge variables overlap. The Magellanic Cloud supergiants appear to have relatively more 10 μm emission, an indication of somewhat more dust at cooler temperatures than in the less massive stars.

The globular cluster stars in Figures 4 or 5 can be divided into two groups: a clump in the lower left whose colors show no evidence for excess infrared emission (and which corresponds to the location of normal, nonvariable field giants) and a sequence extending upward and toward the right. All the LPVs and Pecs that were measured at 10 μm show excess emission while none of the other cluster stars shows a measurable excess. The three Pecs, though, have a smaller excess than the mean for the LPVs. In agreement with the discussion of the previous section, we conclude that among the globular cluster red giants it is only the most luminous pulsating stars—the LPVs—and those that are in quite an advanced evolution state (and also pulsating)—the peculiar variables—that show positive evidence of circumstellar emission and hence a substantial rate of mass loss.

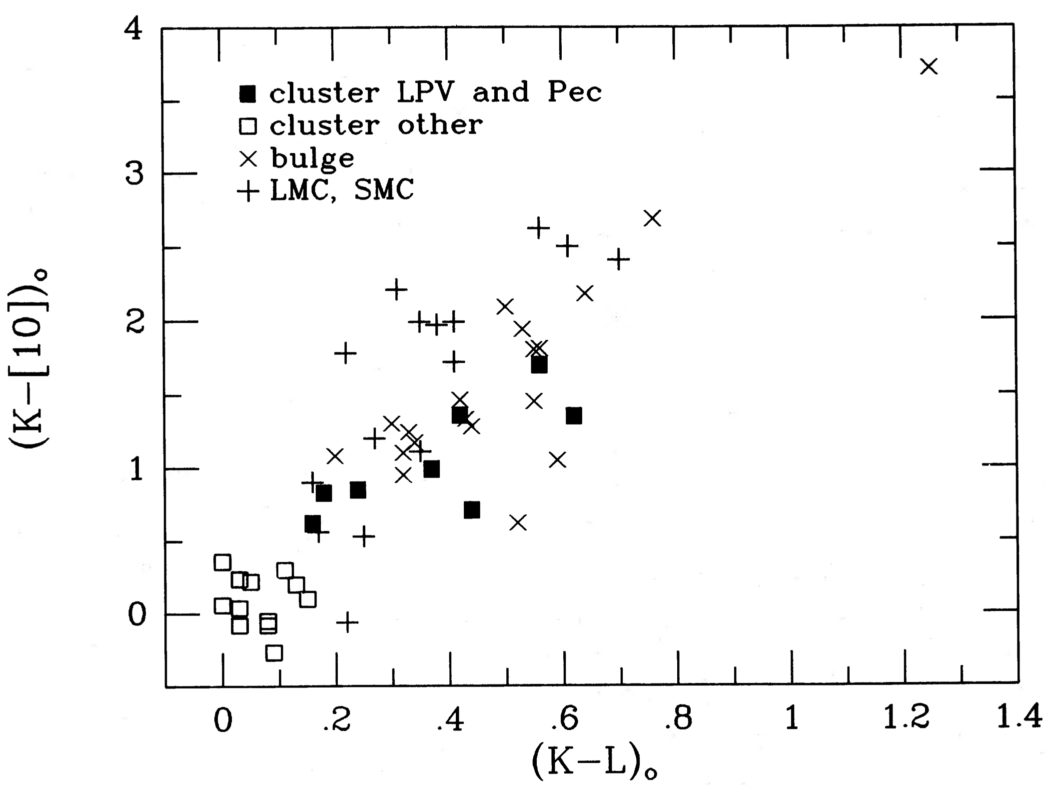

FIG. 4.—$K-[10]$ vs. $K-L$ for globular cluster variables and comparison objects. The 10 μm data are from Tables 1 and 2 of this paper for the globular cluster variables, from Elias, Frogel, and Humphreys (1985) for Magellanic Cloud supergiants, and from Frogel and Whitford (1987, and references therein) for galactic bulge stars.

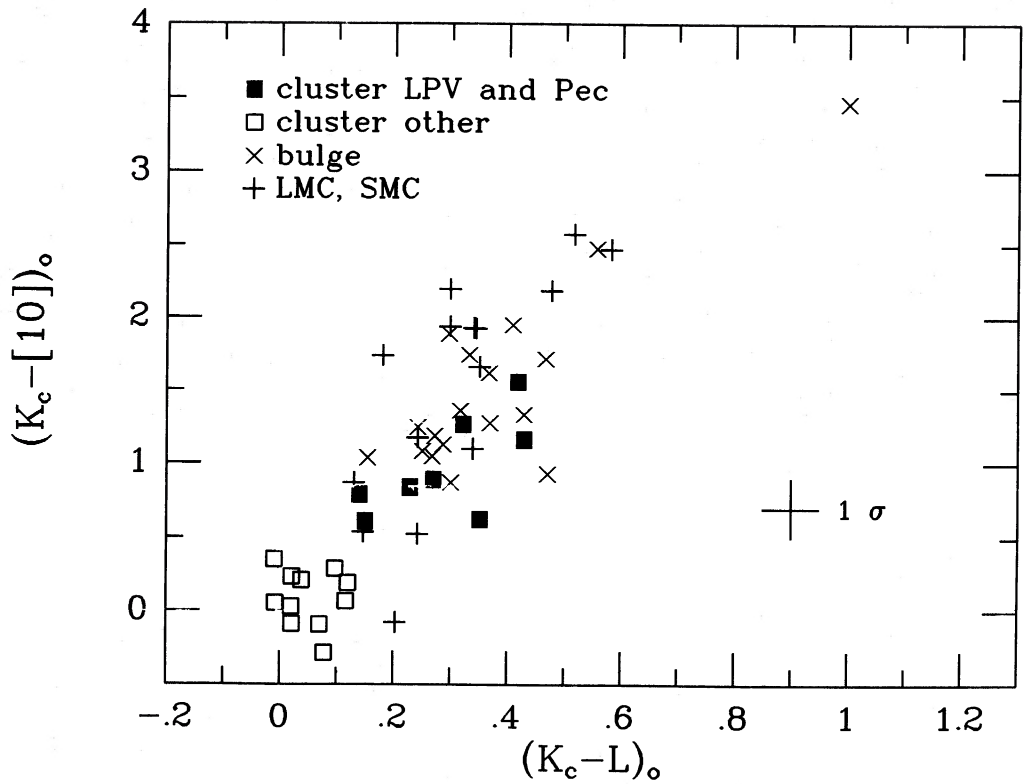

FIG. 5.—Same as Fig. 4 except that the K magnitudes have been corrected for H_2O blanketing. The 1 σ mark reflects uncertainties in the measurements alone, not in the blanketing correction.

V. *JHK* COLORS AND THE EFFECT OF H_2O ABSORPTION

Figures 6, 7, and 8 show, respectively, a $J-H$, $H-K$ plot for the globular cluster variables, the dependence of H_2O on $J-K$ for the same stars, and the dependence of $\Delta(JHK)$ on $\Delta(H_2O)$. The value $\Delta(JHK)$ measures the displacement in magnitudes from the mean field line in Figure 6 along a line of slope $-45°$ while $\Delta(H_2O)$ is the distance in magnitudes above the field line in Figure 7; it is a measure of the excess absorption due to water. Only stars with $\Delta(JHK) > 0.05$, or $\Delta(H_2O) > 0.1$, or with a "pec" designation are included in Figure 8.

Figure 8, with twice as many stars with $\Delta(H_2O) > 0.1$ as the corresponding Figure 4 in the FCP, confirms the main result from that figure and extends it to Δ values nearly twice as large: *absorption by* H_2O *strongly and systematically affects the JHK colors of stars in which it is present.* Many of the small amplitude non–Pec variables in Figure 6 are displaced somewhat from the mean line for globular cluster stars. It is not unreasonable to attribute this to the effects of mild H_2O absorption although other sources of differential blanketing between the variables and nonvariables cannot be ruled out. Even though they have relatively blue colors, half of the Pec variables are displaced redward in $H-K$ from the other small amplitude variables. Inspection of Figures 7 and 8 shows excess H_2O absorption as the likely culprit. The Pec variable with the most extreme H_2O absorption is NGC 6712–V2.

The sequence of variables extending to red $H-K$ colors and high H_2O indices in Figures 6–8 is defined by the LPVs. The two other stars which lie in the same region of Figures 7 and 8 are the possible LPVs (see § III) 47 Tuc V4 and NGC 6352–L36. So, with the lone exception of the Pec variable NGC 6712–V2, the LPVs are separated in both their *JHK* colors and H_2O indices from the rest of the variable stars in globular clusters.[5] Such a separation between LPVs and non-LPVs is also apparent for field stars (Feast *et al.* 1982); an even clearer demarcation exists for stars in the Galactic nuclear bulge (Frogel and Whiteford 1987). The distributions of the field, bulge, and globular cluster LPVs overlap considerably in the $J-H$, $H-K$ diagram despite what must be significant differences in the mean metallicities of the three samples.

Finally, Figure 7 shows a rather sharp cutoff to the $J-K$ colors of the variables of about 1.2. Essentially all of the stars near this limit are LPVs with large H_2O excesses. It is apparent from the detailed observations of 47 Tuc V1–4 that the variation in $J-K$ through a cycle is less than in either $J-H$ or $H-K$, since during a cycle a star generally follows the sequence defined by LPVs in Figure 6. Hence it would be incorrect to attribute the small variations in $J-K$ solely, or even primarily, to variations in T_e. Rather, absorption by H_2O must play an important role in the determination of the $J-K$ colors of LPVs. Effective temperatures determined from a calibration of $J-K$ against T_e from lunar occultation data would need to be corrected for differences in the H_2O absorption between the calibrating stars and the stars in question.

[5] Menzies and Whitelock (1985) note a similar separation in the *JHK* colors for the globular cluster stars in their sample. They suggest, on the basis of a $J-H$, $H-K$ plot that V2 in NGC 362 and V8 in NGC 6712 are similar to LPVs. V8 has been shown to be a Pec variable (Frogel 1985*b*). V2 is not quite bright enough bolometrically to be an LPV, and it also has weak H_2O absorption and rather ordinary *JHK* colors.

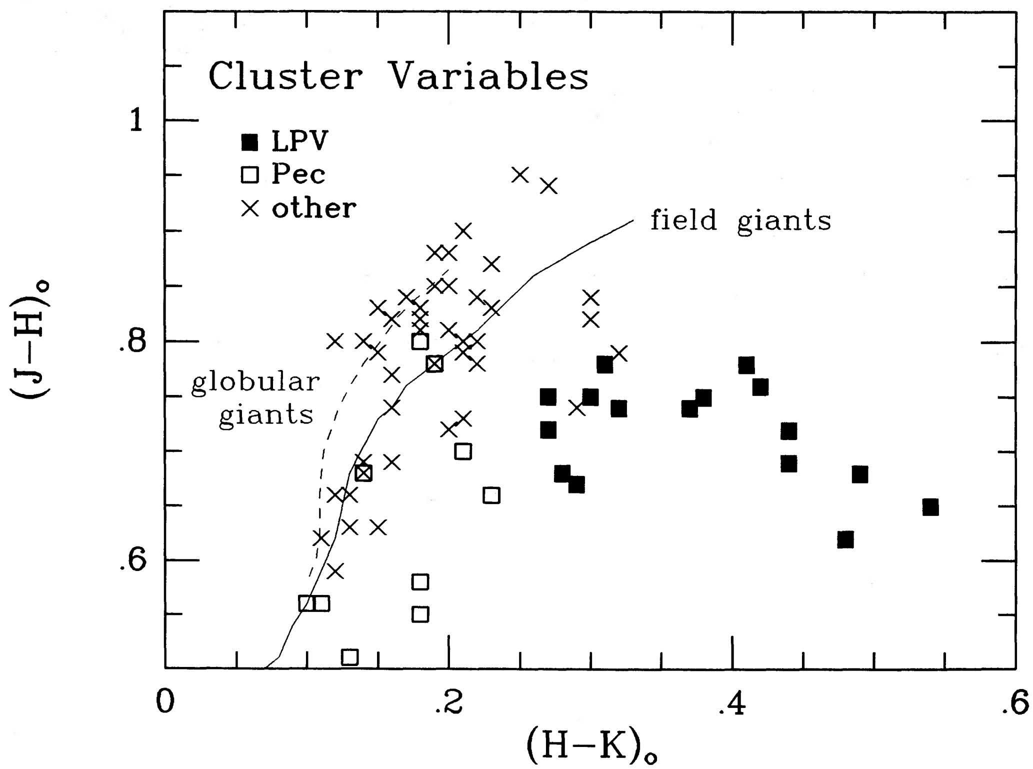

FIG. 6.—$J-H$ vs. $H-K$, as in Fig. 1. The mean line for field giants in the solar neighborhood is from Frogel *et al.* (1978). That for globular cluster giants is from FPC and references therein.

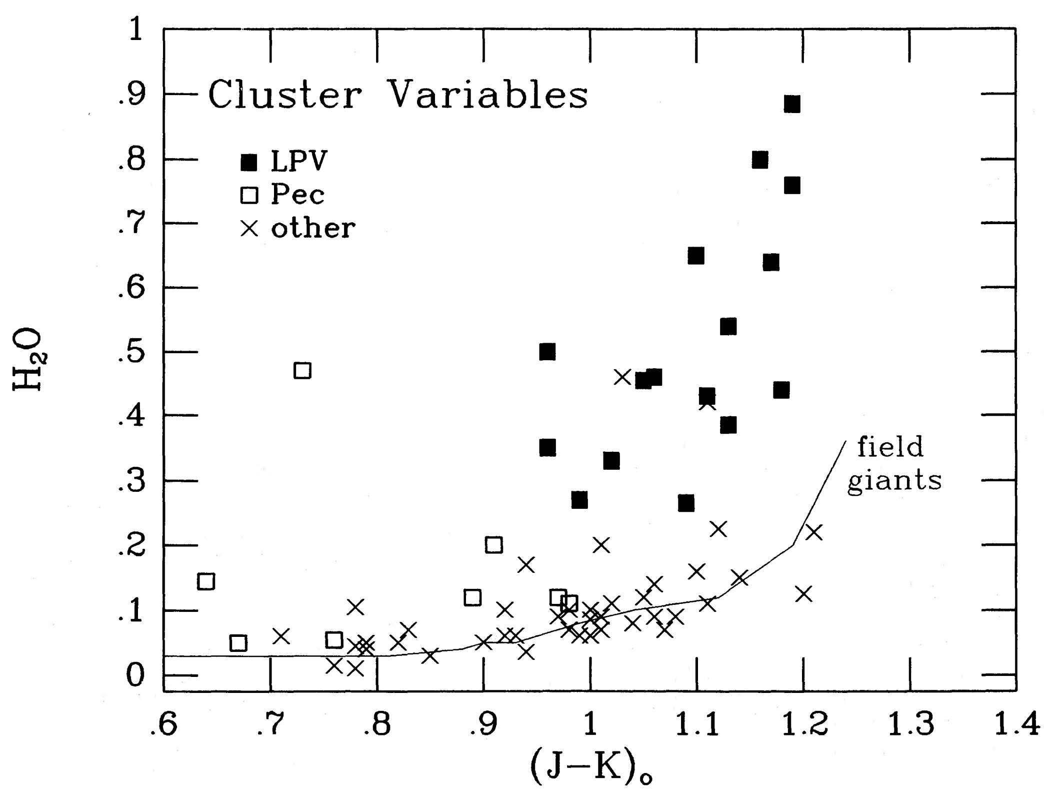

FIG. 7.—H_2O vs. $J-K$ as in Fig. 1. The mean field line is from Aaronson, Frogel, and Persson (1978).

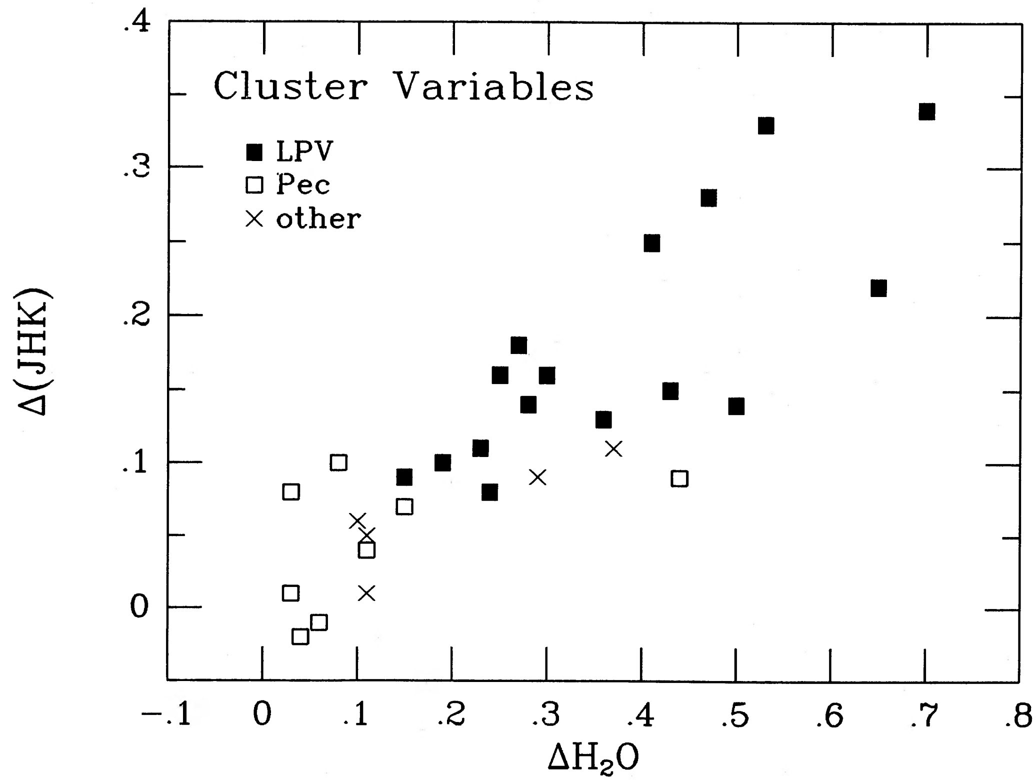

FIG. 8.—$\Delta(JHK)$ vs. $\Delta(H_2O)$ for globular cluster variables—$\Delta(H_2O)$ measures the excess absorption, i.e., the distance of a star above the mean field line in Fig. 7; $\Delta(JHK)$ measures the displacement along a line of slope 45° from the mean line for field giants in Fig. 6. Stars with small displacements in both axes were not plotted in Fig. 8.

VI. CLASSIFICATION OF THE VARIABLES

Long-period variables are easily identified from optical observations alone because of their large light amplitudes and periods. Attention was first drawn to what we call Peculiar variables by Eggen (1972, 1977) and Lloyd Evans (1974, 1983*a*) on the basis of their relatively blue $B-V$ colors. In Paper I NGC 4833–V9 was first identified as a member of this class. Infrared observations revealed two more members in NGC 6712 (Frogel 1985*b*), while the present data confirm the membership of NGC 6388–V8 (Lloyd Evans and Menzies 1973).

As has been demonstrated, infrared colors can separate the cluster LPVs and the Pecs from each other and from the majority of red variables which do not fall into either of these classes. Differences between the infrared characteristics of the three groups arise from significant differences in three physical characteristics: luminosity, temperature, and amount of circumstellar material. The LPVs in particular show little or no overlap with other types of variables. The attempt to label some less luminous variables of smaller amplitude in clusters with $[Fe/H] < -1.0$ as "low metallicity analogues of the LPVs" on the basis of their optical spectra alone is not supported by the present data. No further divisions for the red variables are apparent from the infrared data and any such divisions based purely on optical criteria must be relatively superficial (cf. the discussion by Lloyd Evans 1983*b*).

The main characteristics of the three groups of variables as determined from the infrared data of this paper and Paper I can be summarized as follows:

LPVs:

1. M_{bol} brighter than core He flash.
2. Strong H_2O absorption at 1.9 μm.
3. Substantial excess emission at L.

Peculiar variables:

1. Blue $J-K$ and $V-K$ colors for their M_{bol}.
2. M_{bol} close to but not brighter than core He flash.
3. Moderate H_2O excess absorption for their color.
4. Weak to moderate excess emission at L.

Ordinary variables:

1. M_{bol} fainter than core He flash.
2. Little or no excess emission at L.
3. Little or no excess H_2O absorption.

This is a classification scheme based on easily measured quantities that are directly linked to physical characteristics of the stars and should prove useful in better understanding their evolution.

VII. MASS LOSS AND 10 μm EMISSION

a) Models for the Excess Emission

The excess emission seen in all of the LPVs and many of the peculiar variables at L and beyond is almost certainly due to thermal emission from dust in a circumstellar shell. The excesses in terms of magnitudes are such that the emission must be optically thin (typically, visual optical depths for the stars observed are ~ 0.01) so one would expect narrow-band 10 μm data to show prominently any emission features present in the dust. However, no strong silicate features are seen in the limited data available (Fig. 9), in contrast to higher metallicity galactic field stars (Merrill and Stein 1976). This raises the possibility that there are compositional differences in the grains surrounding cluster and field LPVs.

Since the dust emission is optically thin, we have chosen to use a simple semianalytic model to explore the properties of

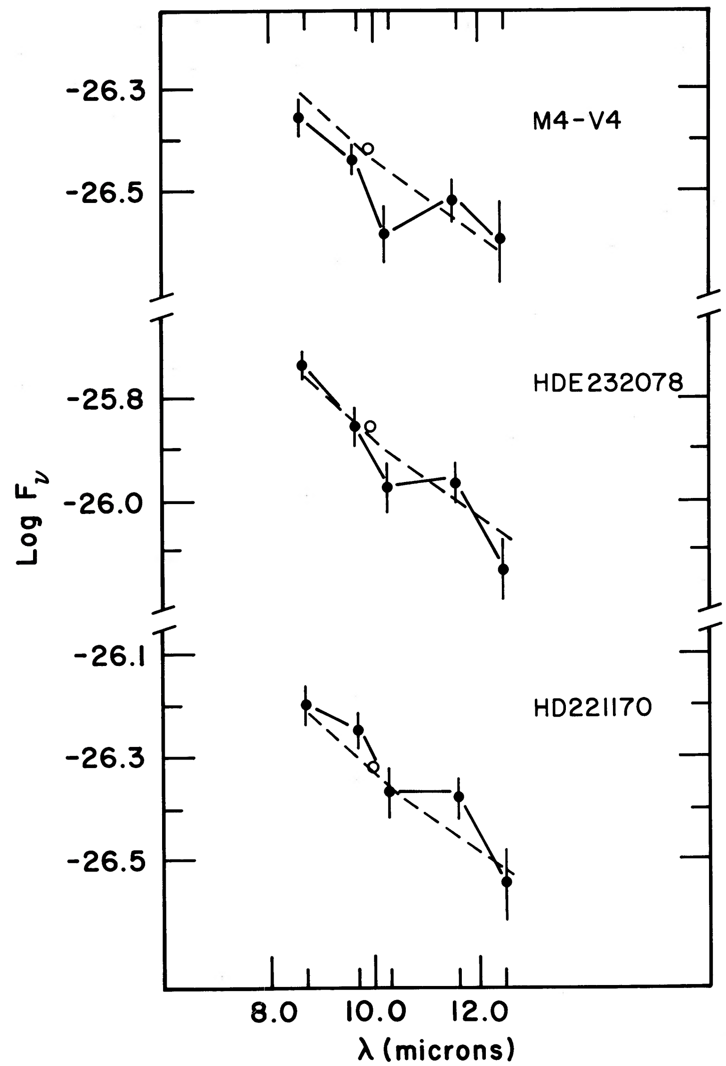

FIG. 9.—Narrow-band 10 μm data for metal-poor stars. No convincing deviation from a smooth continuum is present for any of the stars, although M4–V4 appears redder than a Rayleigh-Jeans distribution.

the dust shell. This choice was dictated primarily by lack of detailed information on dust composition, outflow velocities, and other phyical parameters. However, the form of our model makes it easy to understand the dependence of the results on the various assumptions involved. These results differ only in detail from those of more elaborate calculations (e.g., Hagen 1978).

In our model it is assumed that the infrared excess is due to emission from dust in radiative equilibrium with the central star. The dust shell is assumed to be of sufficiently low optical depth that the radiation emitted or scattered by dust grains and then absorbed by other dust grains can be neglected. The dust is assumed to flow outward from the star at constant velocity, v, so that the dust density is $\propto r^{-2}$, and condense at a temperature T_c. It is assumed that there is some maximum radius of the shell beyond which the dust is too cool to contribute to the observed emission; its precise value is unimportant for the discussion that follows.

The absorption cross section per grain σ_ν at frequency ν is given by

$$\sigma_\nu = Q_{a,\nu} \pi a^2 \tag{2}$$

If the absorption efficiency, $Q_{a,\nu}$, of the dust grains is roughly proportional to grain radius, a, the absorption, κ, per unit mass is then independent of grain size. If κ is roughly proportional to λ^{-1}, and if the stellar effective temperature and radius are T_0 and R_0, then the temperature $T(r)$ of a grain at radius r is

$$T(r) = T_0(R_0/2r)^{2/5} . \tag{3}$$

The emission from the dust in a shell at radius r is then given by

$$dF_\nu(r) = (\dot{M}/v)B_\nu(T)\kappa dr . \tag{4}$$

$\dot{M}$ is the stellar *dust* mass-loss rate, and $B_\nu(T)$ is the emission from a blackbody of temperature $T(r)$. The total emission, F_ν, from the dust shell is then

$$F_\nu = \left(\frac{5h\nu^3}{2c^2}\right) R_0 T_0{}^{5/2} \left(\frac{\dot{M}\kappa}{v}\right) \int_0^{T_c} \frac{T^{7/2}dT}{e^{h\nu/\kappa T} - 1} . \tag{5}$$

This becomes

$$F_\nu = 8.3 \times 10^{-7} \lambda^{-1/2} \dot{M} R_0 T_0{}^{5/2} \kappa/v I(x) \text{ ergs s}^{-1} \text{ sr}^{-1} \text{ Hz}^{-1} , \tag{6}$$

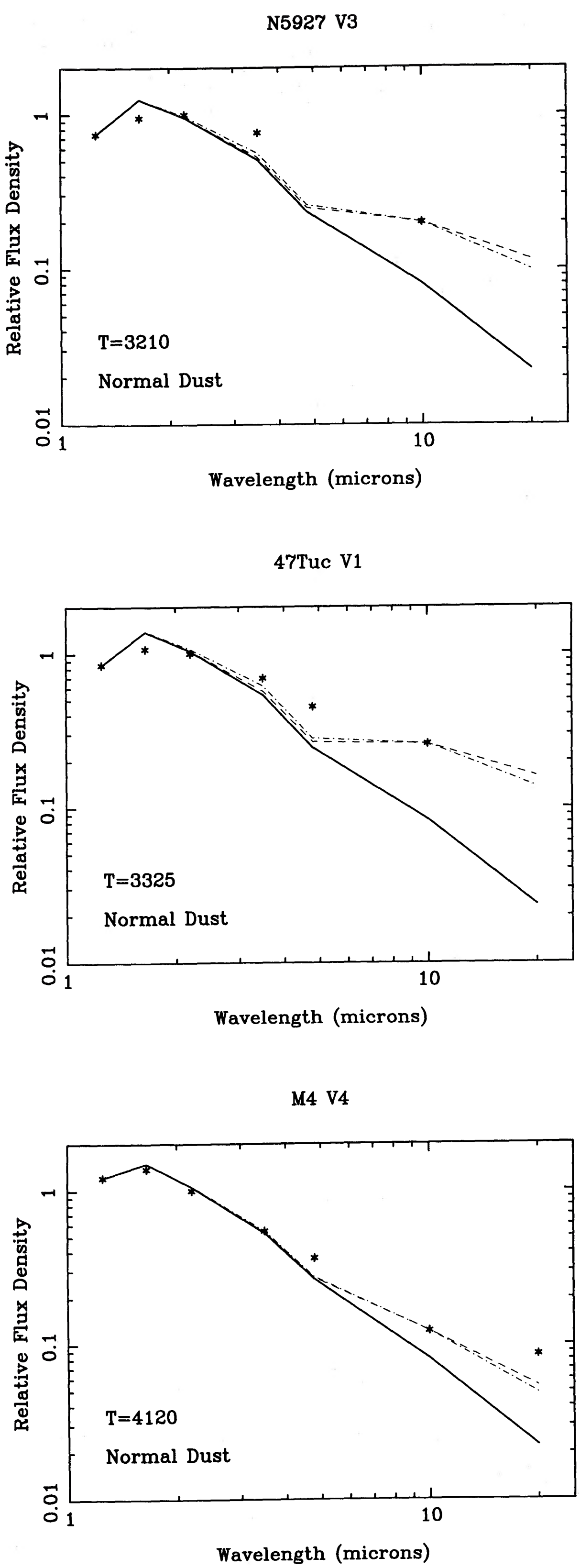

FIG. 10*a*

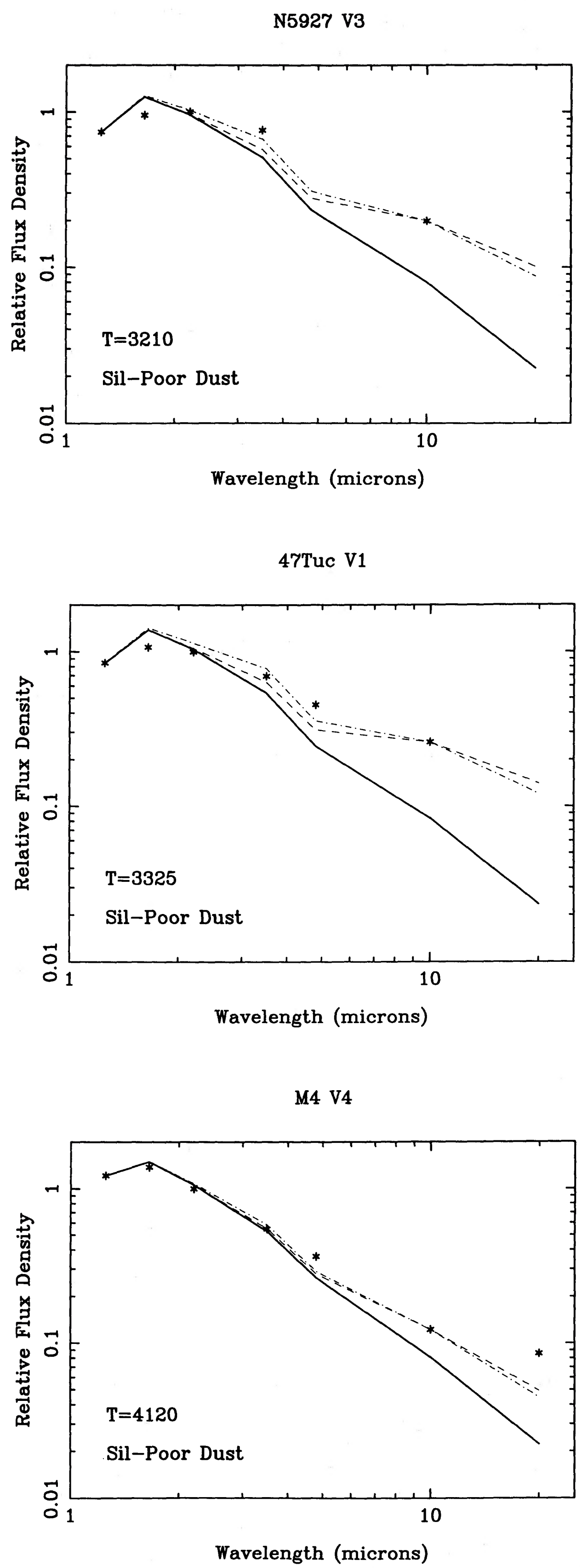

FIG. 10*b*

FIG. 10.—Model fits are shown fr a representative sample of stars using (*a*) "normal" and (*b*) "silicate-poor" dust parameters. Dashed and dot-dashed lines represent fits to the data with dust condensation temperatures of 800 and 1200 K, respectively. Dust mass-loss rates are given in Table 3. Energy distributions have been normalized to the observed flux density at 2.2 μm.

where λ is in μm, $\dot{M}$ in $10^{-10}\ M_\odot\ \mathrm{yr}^{-1}$. R_0 in solar radii, T_0 in K, κ in $\mathrm{cm}^2\ \mathrm{g}^{-1}$, and v in $\mathrm{km\ s}^{-1}$. $I(x)$ is the integral

$$\int_{u_c}^{\infty} \frac{u^{3/2}du}{e^u - 1} \tag{7a}$$

and

$$u_c = h\nu/kT_c\ . \tag{7b}$$

If the condensation temperature T_c is taken as 1000 K (see below), u_c ranges from ~ 0.7 at 20 μm to ~ 6.5 at 2.2 μm. The integral has a value of approximately unity except for large values of the lower limit, u_c, where it becomes small.

For the initial estimates, the grain absorption cross sections were taken from Draine and Lee (1984); the outflow velocity v was taken to be 10 km s^{-1}. The value of T_c can be estimated using the data for the best observed stars with large excess. Examples of fits using differing values of T_c are shown in Figure 10. The heavy solid line is the energy distribution typical of a nonvariable cluster star of the same effective temperature as the variable, normalized at J. Note that the observed H flux is depressed due to the effect of enhanced H_2O absorption in variables as discussed in § V above. The other lines indicate the effects of adding mass loss to the energy distributions. The models are plotted for condensation temperatures T_c of 800 and 1200 K. The mass-loss rate is determined by requiring a fit to the 10 μm data point. There are obvious systematic differences between the model and the data. The discrepancies are that the predicted excess is too small at 3.5 and 4.8 μm when the model is normalized to 10 μm.

Although emission in the model at 10 μm and beyond is largely due to silicates, we have already noted that the limited narrow-band 10 μm data (Fig. 9 and Appendix A) show no sign of the characteristic silicate emission feature. This suggests that silicates may be a less important component in these circumstellar shells than they are in the general interstellar medium (cf. Merrill and Stein 1976); they may not condense as readily as more refractory materials such as graphite.[6] The mass-loss calculations were therefore done for a grain mixture with the contribution of silicates reduced by a factor of 4. The grain mixture, then, changes from roughly half silicate and half graphite (see, Draine and Lee 1984) to 80% graphite and 20% silicate. Fits using the revised grain parameters are shown in Figure 10*b*. The resulting best value of T_c is 1000 ± 200 K, in agreement with the value found by Rowan-Robinson and Harris (1983) for most of their models.[7]. This value has been adopted in the calculations that follow. Model fits such as those shown in Figure 10*b* are used to determine *dust* mass-loss rates for the variables in Tables 1 and 2 with significant 10 μm excesses; these rates are given in Table 3. As may be seen, the graphite-rich mixture yields a dust mass-loss rate a factor of 2 higher than the silicate-rich mixture.

The principal uncertainties in the dust mass-loss estimates are the grain parameters, the condensation temperature, and the outflow velocity. A change in T_c by 200 K causes a change in dM/dt of roughly 15%. A 50% decrease in outflow velocity leads to a halving of dM/dt. Given the possibility of an abnormal grain composition, it is difficult to estimate the effects of uncertainties in the grain parameters. However, in order to bring our mass-loss rates into agreement with predictions from the commonly used Reimers law, the product of grain emissivity and dust-to-gas ratio would have to be increased by a factor greater than 10.[8]

TABLE 3

Mass-Loss Rates

	$\dot{M}_{\mathrm{dust}}(10^{-9}\ M_\odot\ \mathrm{yr}^{-1})$		$\dot{M}_{\mathrm{tot}}(10^{-6}\ M_\odot\ \mathrm{yr}^{-1})$
Star	Normal[a]	Si-Poor[b]	Si-Poor
47 Tuc V1[c]	4.8	9.6	12.3
V2[c]	3.6	7.1	9.1
V3[c]	1.8	3.6	4.6
V4[c]	1.9	3.8	4.9
NGC 4833 V9 ..	0.2	0.4	7.2
NGC 5927 V3 ..	3.4	6.9	3.5
M4 V4[d]	0.5	1.0	5.3
V13	<0.3	<0.6	<3.2
M22 V5	<0.3	<0.6	<8.4
V8	0.4	0.7	9.8
V9	<0.3	<0.6	<8.4
M71 B	0.05	0.1	0.1

[a] Uncertainties are typically ± 0.15 due to placement of stellar continuum, plus 15% due to range of possible T_e values. Upper limits are 3 σ above model fit.

[b] Uncertainties are ± 0.3 plus 15%, as in note a.

[c] Average values used.

[d] IRTF values used.

From the dust-mass-loss rates, *total* mass-loss rates for stars can be estimated. The gas-to-dust mass ratio has been assumed to be proportional to metallicity. For solar metallicity stars and normal dust composition it has been taken to be 160 (Knapp 1985); for solar metallicity stars and the silicate-depleted composition used in the model fits this number becomes 250. Estimates for the total mass-loss rate are given in the last column of Table 3. For these metal-poor stars a measurable 10 μm excess requires a dust mass-loss rate of at least $3 \times 10^{-10}\ M_\odot\ \mathrm{yr}^{-1}$ corresponding to a total mass-loss rate in excess of $10^{-7}\ M_\odot\ \mathrm{yr}^{-1}$. Rates this high or higher are obviously sustainable for only a relatively brief period of a star's evolution—10^6 yr or less—since typical envelope masses for globular cluster red giants are on the order of 0.1 $M_\odot$.

From Table 3 we see that the infrared excesses observed at 3.5 and 10 μm in the globular cluster LPVs imply a total mass-loss rate of $7 \times 10^{-6}\ M_\odot\ \mathrm{yr}^{-1}$ for a typical [Fe/H] of -0.7 and an outflow velocity of 10 km s^{-1}. Although this mass-loss rate is nearly a factor of 10 higher than the mean value of dM/dt for the 7 well-known (non-IR identified) Me

[6] It is worth keeping in mind a more speculative possibility: the 4.8 μm filter is strongly affected by the CO fundamental vibrational transition band, and it is possible that in an extended atmosphere this could be seen more weakly in absorption, or even in emission, as compared with the nonvariable globular cluster stars. Such a possibility could be verified by spectroscopy at 4.7 μm.

[7] Rowan-Robinson and Harris (1983) were able to achieve good fits with their model that used dirty silicate grains. However, we point out that all of the stars they fit most likely have solar metallicity or greater.

[8] The referee has suggested that the absence of the silicate feature is a piece of "quite convincing evidence against the presence of significant amounts of circumstellar dust." Rather, the referee prefers the explanation that the excess emission is due to a much cooler photospheric temperature than we assume. We have argued against this alternative explanation in an earlier section. What we have done in calculating the models is to correct the $J-K$ color of the star we are fitting for H_2O absorption and then match its energy distribution up to that of a nonvariable of the same effective temperature as judged by the $J-K$ color. Temperatures are estimated by looking at the relative shifts in blackbody colors for a shift in temperature. This is not ideal, but appears to be the best we can do with limited knowledge. We estimate the uncertainty in the resulting mass-loss rates from the uncertainty in the stellar effective temperature to be no greater than any of the other sources of uncertainty.

Miras from Table 1 of Knapp (1985), it lies near the midpoint of the range of values derived by Wannier and Sahai (1986) for other cool M stars in the solar neighborhood. Our new values are nearly a factor of 50 larger than those which would be calculated if the Reimers (1975) relation were applied to these stars (cf. Frogel 1983). Using a somewhat different approach and with the longer wavelength *IRAS* data as a basis, Gillett *et al.* (1987) also derive rather high (but still lower than ours) values for stars in 47 Tucanae. We emphasize that our estimate (and Gillett *et al.*'s) is independent of the *sources* of energy that drives the outflow, but depends only on the assumptions that have gone into modeling the emission itself.

b) Further Considerations

If we assume that *relative* mass-loss rates determined from the same modeling procedure have less uncertainty than the absolute rates, it is clear that LPVs which have been initially identified via infrared searches have mass-loss rates typically 10 times greater than those of solar neighborhood optical LPVs (see, e.g., Knapp 1985; Knapp and Morris 1985). The lifetimes of the "infrared" LPVs must indeed be short and they must be very near the end of their lives as red giants. We propose that the absence of such objects in globular clusters is due to their short lifetimes (i.e., low frequency of occurrence) compared with normal LPVs and the fact that the relatively low metallicity of the globular cluster giants means that these latter stars will have less massive envelopes and will not be able to evolve to as high a luminosity on the giant branch as more metal-rich objects (VandenBerg and Laskarides 1987). As Wood, Bessell, and Fox (1983, and references therein) have proposed, it is evolution to high luminosities on the asymptotic giant branch that permits an LPV to switch from first-overtone to fundamental mode pulsation with a resultant high mass-loss rate and rapid loss of the stellar envelope.

Excess emission at 3.5 and 10 μm is closely correlated with strong H_2O absorption (Figs. 3 and 5). Since H_2O absorption is strongly temperature-dependent in cool stars (see, e.g., Frogel 1971; Baldwin, Frogel, and Persson 1973, and Aaronson, Frogel, and Persson 1978; laboratory measures of the emissivity of hot H_2O may be found in Ferriso and Ludwig 1964), the correlation between infrared excess and H_2O suggests that a circumstellar shell is associated with a more extended atmosphere and more material at lower temperatures than is found in stars without such a shell. It is not surprising that the effect is strongest in LPVs since their relatively high luminosity coupled with the kinetic energy available from pulsation could supply the energy required to create a more extended atmosphere and a circumstellar shell. The extended, cool atmosphere would further enhance a star's ability to form grains.

There is theoretical support for this line of reasoning. Wood (1979) finds that pulsations by themselves contribute only weakly to the mass loss from a star. However, if there already exists a steady mass outflow such as might be caused by radiation pressure on grains, Wood calculates that a pulsating atmosphere at the base of such an outflow will increase dM/dt by *a factor of 40* which, coincidentally, is the enhancement we find over that predicted from the Reimers relation based primarily on nonpulsating stars. At the same time, according to Wood, the steady-state flow velocity far from the star will change only slightly from its value in the absence of pulsation. Jones, Ney, and Stein (1981) also argue that pulsation can increase the mass-loss rate over that calculated from radiation pressure on dust alone by several orders of magnitude because of a large increase in the atmospheric scale height.

We would expect a higher mass-loss rate to result in a denser circumstellar shell and stronger infrared excess emission in LPVs of similar mass and luminosity. Such an expectation is consistent with the clear separation observed between photometrically determined parameters for large amplitude pulsators, i.e., the LPVs, and for the rest of the stars in metal-poor, solar abundance, and metal-rich stellar populations (e.g. Glass and Feast 1982*a*, *b*; Feast, *et al.* 1982; Menzies and Whitelock 1985; Frogel 1985*a*; Frogel and Whitford 1987). A preliminary analysis of ground-based infrared observations and of data from the *Infrared Astronomical Satellite* for 18 LPVs (Whitelock, Pottasch, and Feast 1986) does indeed show a relationship between dust shell mass, pulsation amplitude, and luminosity.

Jura (1984) finds that while there may be some mass loss from chromospheric activity or pulsation if no dust grains are present, the formation of dust leads to a significant enhancement of dM/dt. He also remarks that pulsations can act to raise matter above the photosphere into cooler regions thus enhancing the dust formation rate (Jura 1986). Similarly, Knapp (1986) finds strong evidence for "the hypothesis that the [stellar] winds derive most of their momentum from radiation pressure [on the dust grains]." These arguments suggest that metal-poor stars should have lower mass-loss rates than metal-rich stars, other things being equal. Our analysis shows, however, that mass-loss rates in globular cluster LPVs are comparable to those in field LPVs of considerable higher metallicity. Furthermore, differences in luminosity between the brightest non–LPV giants and the LPVs in the globular clusters fall short of being large enough to account for the much greater infrared excesses observed in the latter stars than in the former. We also comment that in Baade's window there is considerable overlap in luminosity between LPVs and non-LPVs (Frogel and Whitford 1987), yet it is only the LPVs that show significant amounts of excess emission at 3.5 and 10 μm. We conclude, then, the pulsation plays an important and perhaps dominant role in determining mass-rates for low-mass stars.[9]

VIII. SUMMARY AND CONCLUSIONS

The main results of this study are that the long-period and peculiar variables in globular clusters define classes of stars distinct from the other stars in the clusters. They are defined by unique characteristics, which are presumably physically related. Second, the mass-loss rates deduced for the cluster LPVs are comparable to those calculated for metal-rich solar neighborhood stars with significantly greater infrared excesses. This implies that pulsation plays a key role in deriving the mass loss.

The characteristics of the variables are the following.

1. High luminosity. Without exception the LPVs have luminosities above that required for core helium flash. They

[9] Fusi-Pecci and Renzini (1975*a*, *b*) address the problem of how to get mass loss in metal-poor stars. Their solution is to use energy from acoustic waves in the convective region of a red giant's atmosphere as a substitute for radiation pressure on grains. The amount of energy in these acoustic waves decreases with increasing Z faster than the decrease in surface gravity potential so that at some point radiation pressure on grains take over. The required efficiency of their process in low Z stars must be comparable to that seen in the Sun in order to get a mass-loss rate high enough to account for the morphology of globular clusters horizontal branches.

TABLE 4

IRTF OBSERVATIONS OF NGC STARS AND FIELD STARS

	Photometry from the IRTF[a]										
Star	B-V	K	V-K	J-K	H-K	K-L	K-M	K-N	K-Q	M_{bol}	T_e
72	1.53	6.56	3.45	0.88	0.16	0.12	-0.03 (6)	-0.22 (10)	...	-2.22	4000
193	1.14	9.13	2.49	0.62	0.11	0.09	...	0.39 (38)	...	-0.06	4650
304	1.45	6.69	3.39	0.89	0.14	0.09	-0.30 (8)	0.16 (12)	...	-2.11	4020
329	1.14	8.72	2.60	0.66	0.10	0.07	...	<0.27	...	-0.41	4470
461	1.36	7.22	3.10	0.80	0.13	0.09	...	0.14 (14)	...	-1.69	4180
494	1.46	6.00	3.73	0.92	0.17	0.14	-0.17 (6)	-0.01 (10)	...	-2.70	3900
501	1.46	6.99	3.21	0.82	0.14	0.11	-0.14 (8)	0.06 (11)	...	-1.88	4120
669	1.38	7.45	3.02	0.79	0.13	0.10	...	0.09 (13)	...	-1.49	4210
751	1.56	6.17	3.70	0.92	0.16	0.12	-0.20 (6)	0.02 (11)	...	-2.54	3920
977	1.49	6.65	3.39	0.87	0.15	0.12	-0.14 (7)	0.09 (11)	...	-2.15	4020
Reddening	0.28	0.09	0.88	0.17	0.06	0.04	0.06	0.07	...	...	...
HD165195	...	4.04	...	0.79	0.16	0.08	-0.06	0.05	1.31 (25)	...	...
HD221170	...	4.86	...	0.67	0.10	0.11	0.06	0.14	-0.02 (24)	...	...
HDE232078	...	3.91	...	1.05	0.19	0.14	0.13	0.32	0.73 (26)	...	...

[a] For the NGC 7789 stars the reddening values tabulated have been applied to the observed values based on $E(B-V)_0 = 0.31$ (Twarog and Tyson 1985). The BV photometry is from the photoelectric data of Burbidge and Sandage 1958. M_{bol} and T_e have been calculated as in FCP with $(m-M)_0 = 11.3 \pm 0.3$ (Twarog and Tyson 1985).

Numbers in parentheses are uncertainties in units of hundredths of a magnitude when greater than 0.05 in $K-L$ and $K-M$ and 0.10 in $K-N$. Uncertainties in the other colors are 0.03 mag or less.

For the HD stars the observed, uncorrected, values are given.

are the only cluster stars to be so luminous. The difficulty of reconciling their luminosities with their ages has been discussed in Paper I. Eighty percent of the peculiar variables have luminosities within 0.2 mag of the top of the first giant branch. Are they the precursors of the LPVs in the metal-rich clusters? Perhaps in the metal-poor clusters insufficient envelope mass is left to allow them to evolve any further in luminosity.

2. Excess infrared emission. Nearly all LPVs and peculiar variables have excess infrared emission at 3.5 μm and beyond, indicative of high mass-loss rates. With only a few, probably misclassified exceptions, no other globular cluster stars show such excess emission.

3. Excess H_2O absorption in the atmospheres. This is interpreted as indicating the presence of additional material in the upper, cooler layers of the stellar atmospheres and/or of more cooler material in general. In either case, it is an illustration of significant differences in the structure of the outer atmosphere of the variable stars as compared with the nonvariables. The strength of the H_2O absorption correlates well with the strength of the circumstellar shell and hence the inferred rate of mass loss. Theoretical studies of the effect of pulsation on mass loss driven by radiation pressure on grains are consistent with the qualitative picture we have presented.

Portions of this work were done while the authors were on the staff at CTIO. We are grateful to the IRTF and to CTIO for allocations of observing time. J. A. F. acknowledges an informative conversation with G. Knapp and many hours of discussion about LPVs with the staff of the SAAO in Cape Town while on a visit there. We appreciate useful suggestions on clarifications to the manuscript by Ed Olszewski. Caty Pilachowski informed us about some unpublished results relevant to the discussion in the Appendix. Some of J. H. E.'s work was supported by the NSF under grant AST83-12699.

APPENDIX

RELATED OBSERVATIONS OF GALACTIC STARS

In addition to the globular cluster stars, a number of galactic stars were measured on the IRTF. These fell into two groups: one, giant branch stars in the open cluster NGC 7789; the other, a few metal-poor field giants which showed Hα emission indicative of possible mass loss. The observations are summarized in Table 4 in a format similar to those of Tables 1 and 2. Star identifications and optical photometry are from Burbidge and Sandage (1958). A selection of the reddest and brightest stars in the cluster were observed. Two of them, 304 and 977, do not appear to be members according to the proper motion study of McNamara and Solomon (1981). (C. Pilachowski has informed us that star 193 in Table 4 is in fact MS No. 388; it too is not a member.) The cluster has a metallicity of [Fe/H] $= -0.25 \pm 0.10$ and an age of $1.6 \pm 0.5 \times 10^9$ yr (Twarog and Tyson 1985). The near-infrared data will be discussed more fully in a later paper.

The field giants are presumably galactic analogs of the globular cluster stars. As they are significantly brighter than the globular cluster stars—by 1–2 mag—they provided the opportunity to make more precise 20 μm and narrow-band 10 μm measurements. Of the three stars, only HDE 232078 shows a convincing excess at 10 μm. (The 20 μm excess for HD 165195 is significant only at the 2.5 σ level.) The narrow-band 10 μm data for HDE 232078 show its spectrum to be essentially featureless like that of NGC 6121–V4. The spectrum of HD 221170, which has no 10 μm excess, is also featureless. This provides further evidence that the grains in these stars are not dominated by silicates. According to Pilachowski (1987) HD 221170 has never shown optical emission lines; emission comes and goes in HD 165195; and HD 23078 always has emission. These results are consistent with the infrared findings.

The NGC 7789 stars are young, more massive, and more metal-rich than any of the other stars considered in this paper but they are not as luminous. The absence of pronounced infrared excesses in these stars confirms that the mass-loss rates are not simple functions of mass, luminosity, and temperature: the presence or absence of pulsation must play a key role. These stars have the same low mass-loss rates as nonvariable globular cluster stars. It should also be noted that the $K-M$ colors of the NGC 7789 stars are uniformly negative with typical values of roughly -0.2. This is presumably due to the relatively high metal abundance in these stars, and to the correspondingly strong CO fundamental at 4.7 μm. Typical $K-M$ colors for field stars and globular cluster stars without an infrared excess are in the range 0.0 to -0.1.

REFERENCES

Aaronson, M., Frogel, J. A., and Persson, S. E. 1978, *Ap. J.*, **220**, 442.
Baldwin, J. R., Frogel, J. A., and Persson, S. E. 1973, *Ap. J.*, **184**, 427.
Burbidge, E. M., and Sandage, A. 1958, *Ap. J.*, **128**, 174.
Clement, C. C., and Hogg, H. S. 1977, *A.J.*, **82**, 968.
Cohen, J. G. 1976, *Ap. J. (Letters)*, **203**, L127.
Draine, B. T., and Lee, H. M. 1984, *Ap. J.*, **285**, 89.
Dupree, A. K., Hartmann, L., and Avrett, E. H. 1984, *Ap. J. (Letters)*, **281**, L37.
Eggen, O. J. 1972, *Ap. J.*, **213**, 767.
———. 1977, *Ap. J.*, **213**, 767.
Elias, J. H., Frogel, J. A., and Humphreys, R. M. 1985, *Ap. J. Suppl.*, **57**, 91.
Elias, J. H., Frogel, J. A., Matthews, K., and Neugebauer, G. 1982, *A.J.*, **87**, 1029.
Feast, M. W. 1973, in *IAU Colloquium 21, Variable Stars in Globular Clusters and Related Systems*, ed. J. D. Fernie (Dordrecht: Reidel), p. 131.
Feast, M. W. 1985, *Mem. Soc. Astr. Italiana.*, **56**, 213.
Feast, M. W., Robertson, B. S. C., Catchpole, R. M., Lloyd Evans, T., Glass, I. S., and Carter, B. S. 1982, *M.N.R.A.S.*, **201**, 439.
Ferriso, C. C., and Ludwig, C. B. 1964, *J. Chem. Phys.*, **41**, 1668.
Frogel, J. A. 1971, Ph.D. thesis, California Institute of Technology.
———. 1983, *Ap. J.*, **272**, 167 (Paper I).
———. 1985*a*, *Mem. Soc. Astr. Italiana*, **56**, 193.
———. 1985*b*, *Ap. J.*, **291**, 581.
Frogel, J. A., Cohen, J. G., and Perrson, S. E. 1983, *Ap. J.*, **275**, 789 (FCP).
Frogel, J. A., Persson, S. E., Aaronson, M., and Matthews, K. 1978, *Ap. J.*, **220**, 75.
Frogel, J. A., Persson, S. E., and Cohen, J. G. 1981, *Ap. J.*, **246**, 842.
———. 1983, *Ap. J. Suppl.*, **53**, 713 (FPC).
Frogel, J. A., and Whitford, A. E. 1987, *Ap. J.*, **320**, 199.
Fusi-Pecci, F., and Renzini, A. 1975*a*, in *Proc. 19th International Astrophysics Symposium, Liège*, p. 383.
———. 1975*b*, *Astr. Ap.*, **39**, 413.
Gillett, F. C., de Jong, T., Neugebauer, G., Rice, W. L., and Emerson, J. P. 1987, *Ap. J.*, submitted.
Glass, I. S., and Feast, M. W. 1982*a*, *M.N.R.A.S.*, **198**, 199.
———. 1982*b*, *M.N.R.A.S.*, **199**, 245.
Hagen, W. 1978, *Ap. J. Suppl.*, **38**, 1.
Harris, H. C. 1987, in *Stellar Pulsation*, ed. A. N. Cox and W. M. Sparks, in press.
Hogg, H. S. 1973, *Pub. David Dunlop Obs.*, **3**, No. 6.
Humphreys, R. M., Jones, T. J., and Sitko, M. 1984, *A.J.*, **89**, 1155.
Jones, T. J., Hyland, A. R., and Robinson, G. 1984, *A.J.*, **89**, 999.
Jones, T. W., Ney, E. P., and Stein, W. A. 1981, *Ap. J.*, **250**, 324.
Jura, M. 1984, *Ap. J.*, **282**, 200.
———. 1986, *Ap. J.*, **303**, 327.

Knapp, G. R. 1985, *Ap. J.*, **293**, 273.
———. 1986, *Ap. J.*, **311**, 731.
Knapp, G. R., and Morris, M. 1985, *Ap. J.*, **292**, 640.
Lloyd Evans, T. 1974, *M.N.R.A.S.*, **167**, 393.
———. 1983*a*, *M.N.R.A.S.*, **204**, 945.
———. 1983*b*, *M.N.R.A.S.*, **204**, 961.
———. 1984, *M.N.R.A.S.*, **209**, 825.
Lloyd Evans, T., and Menzies, J. W. 1973, in *IAU Colloquium 21, Variable Stars in Globular Clusters and Related Systems*, ed. J. D. Fernie (Dordrecht: Reidel), p. 151.
Lloyd Evans, T., and Menzies, J. W. 1977, *M.N.R.A.S.*, **178**, 163.
Mallia, E. A., and Pagel, B. 1981, *M.N.R.A.S.*, **194**, 421.
McNamara, B. J., and Solomon, S. 1981, *Astr. Ap. Suppl.*, **43**, 333.
Menzies, J. W., and Whitelock, P. A. 1985, *M.N.R.A.S.*, **212**, 783.
Merrill, K. M., and Stein, W. A. 1976, *Pub. A.S.P.*, **88**, 285.
Payne-Gaposchkin, C., and Gaposchkin, S. 1938, *Harvard Observatory Monographs, No. 5, Variable Stars* (Cambridge: Harvard Observatory).
Pickering, E. C. 1881, *Proc. Amer. Acad. Arts Sciences*, **16**, 17.
Pilachowski, C. 1987, private communication.
Reimers, D. 1975, in *Proc. 19th International Astrophysics Symposium, Liège*, p. 369.
Rich, R. M. 1986, Ph.D. thesis, California Institute of Technology
Rowan-Robinson, M., and Harris, S. 1983, *M.N.R.A.S.*, **202**, 767.
Sandage, A., Smith, L. L., and Norton, R. M. 1966, *Ap. J.*, **144**, 894.
Sweigart, A. V., and Gross, P. G. 1978, *Ap. J. Suppl.*, **36**, 405.
Twarog, B. A., and Tyson, N. 1985, *A.J.*, **90**, 1247.
VandenBerg, D., and Laskarides, P. G. 1987, *Ap. J. Suppl.* **64**, 103.
Wannier, P. G., and Sahai, R. 1986, *Ap. J.*, **311**, 335.
Welty, D. E. 1985, *A.J.*, **90**, 2555.
Whitelock, P. A. 1986, *M.N.R.A.S.*, **219**, 525.
Whitelock, P. A., Feast, M. W., and Catchpole, R. M. 1986, *M.N.R.A.S.*, **222**, 1.
Whitelock, P. A., Pottasch, S. R., and Feast, M. W. 1987, Proceedings of the Calgary Workshop on Cool Stars, in press.
Whitford, A. E., and Rich, R. M. 1983, *Ap. J.*, **274**, 723.
Wood, P. R. 1979, *Ap. J.*, **227**, 220.
Wood, P. R., and Bessell, M. S. 1983, *Ap. J.*, **265**, 748.
Wood, P. R., Bessell, M. S., and Fox, M. W. 1983, *Ap. J.*, **272**, 99.
Zinn, R., and West, M. J. 1984, *Ap. J. Suppl.*, **55**, 45.

J. H. ELIAS: Cerro Tololo Inter-American Observatory, P.O. Box 26732, 950 North Cherry Avenue, Tucson, AZ 85726

J. A. FROGEL: Kitt Peak National Observatory, P.O. Box 26732, 950 North Cherry Avenue, Tucson, AZ 85726